Fragmentation of electric dipole strength in $N = 82$ isotones

Mitsuru Tohyama[1] and Takashi Nakatsukasa[2,3]

[1]*Kyorin University School of Medicine, Mitaka, Tokyo 181-8611, Japan*
[2]*RIKEN Nishina Center, Wako, Saitama 351-0198, Japan*
[3]*Center for Computational Sciences, University of Tsukuba, Tsukuba 305-8571, Japan*

Fragmentation of the dipole strength in the $N = 82$ isotones ^{140}Ce, ^{142}Nd, and ^{144}Sm is calculated using the second random-phase approximation (SRPA). In comparison with the result of the random-phase approximation (RPA), the SRPA provides additional damping of the giant dipole resonance and the redistribution of the low-energy dipole strength. Properties of the low-energy dipole states are significantly changed by the coupling to two-particle–two-hole (2p-2h) states, which are also sensitive to the correlation among the 2p-2h states. Comparison with available experimental data shows a reasonable agreement for the low-energy $E1$ strength distribution.

The low-energy dipole states, often referred to as the pygmy dipole resonance (PDR), have attracted recent experimental [1–7] and theoretical interest [8–13] (see also the recent review [14] and references therein). These states are also of significant astrophysical interest, since the low-energy dipole strengths close to the neutron threshold strongly affect the astrophysical r-process nucleosynthesis [15].

The quasiparticle random-phase approximation based on the Hartree-Fock-Bogoliubov ground state (HFB+QRPA) has been extensively used to study the PDRs as well as the giant dipole resonances (GDRs). Recent systematic calculations [16] for the Nd and Sm isotopes show that although the HFB+QRPA nicely reproduces characteristic features of the shape phase transition in the GDR, it fails to produce the low-energy dipole strengths at $E_x = 5.5$–8 MeV, observed in the $N = 82$ isotones, ^{142}Nd and ^{144}Sm [1,3]. The disagreement suggests that the coupling to complex configurations, such as multiparticle-multihole states, is required to study the PDRs in these nuclei. In fact, the quasiparticle-phonon model (QPM), which takes into account coupling to multiphonon states, successfully reproduces the low-energy dipole strengths in the $N = 82$ nuclei [2,4]. A similar approach based on the relativistic mean-field model has also been used to study the PDRs in the tin and nickel isotopes [17]. These models assume the multiphonon characters of the complex states and violate the Pauli principle. Thus, it is desirable to study properties of the PDRs with a method complementary to these phonon-coupling approaches. In this work, we present studies for the dipole excitations in the $N = 82$ isotones, with the second random-phase approximation (SRPA) (Ref. [18] and references therein). The SRPA explicitly incorporates the two-particle–two-hole (2p-2h) states instead of "two-phonon" states and respects the Pauli principle in the 2p-2h configurations. Recently, the low-energy dipole states in ^{40,48}Ca have been studied with the SRPA [19], which suggests that the coupling between one-particle–one-hole (1p-1h) and 2p-2h configurations enhances the electric dipole ($E1$) strength in the energy range from 5 to 10 MeV. We investigate whether a similar effect can be observed in the isotones of $N = 82$. Since there are many dipole states with small $E1$ strengths in

the energy region below 8 MeV, it is difficult to compare the properties of each state with the experiment. Thus, we perform a comparison of integrated properties at low energies.

The SRPA equation is written in the matrix form [18]

$$\begin{pmatrix} a & c \\ b & d \end{pmatrix} \begin{pmatrix} x^\mu \\ X^\mu \end{pmatrix} = \omega_\mu \begin{pmatrix} x^\mu \\ X^\mu \end{pmatrix}, \qquad (1)$$

where x^μ_{ph} and $X^\mu_{pp'hh'}$ ($p \leftrightarrow h$) are the 1p-1h and 2p-2h transition amplitudes for an excited state with an excitation energy ω_μ. The explicit expression for the matrices a, b, c, and d are given in Ref. [20].

The Skyrme interaction of the SIII parameter set is used to calculate the Hartree-Fock single-particle states. The continuum states are discretized by confining the single-particle wave functions in a sphere of radius of 20 fm. We have confirmed that the $E1$ strength distribution is not significantly affected by the adopted box size. Single-particle states with angular momenta $j_\alpha \leqslant 15/2$ up to 30 MeV in energy ($\epsilon_\alpha < 30$ MeV) are adopted for the 1p-1h space (x^μ_{ph} and x^μ_{hp}), both for protons and neutrons. This roughly amounts to 100 single-particle states. For the 2p-2h amplitudes ($X^\mu_{pp'hh'}$ and $X^\mu_{hh'pp'}$), we truncate the space into the one made of the single-particle states near the Fermi level, the $2p_{3/2}$, $2p_{1/2}$, $1g_{9/2}$, $1g_{7/2}$, $2d_{5/2}$, $2d_{3/2}$, $3s_{1/2}$, $1h_{11/2}$, and $1h_{9/2}$ orbits for protons and the $2d_{5/2}$, $2d_{3/2}$, $1h_{11/2}$, $1h_{9/2}$, $2f_{7/2}$, and $1i_{13/2}$ orbits for neutrons. The proton orbits up to the $1g_{7/2}$ orbit are assumed to be fully occupied in the ground state of ^{140}Ce, while the proton $2d_{5/2}$ orbit is assumed to be partially occupied in the ground states of ^{142}Nd and ^{144}Sm. The numbers of 1p-1h and 2p-2h amplitudes in the SRPA are about 800 and 9000, respectively.

For calculation of the SRPA matrix elements, we employ a residual interaction of the t_0 and t_3 terms of the SIII interaction. Since the residual interaction is not fully consistent with the one used in the calculation of the single-particle states, it is necessary to adjust the strength of the residual interaction so that the spurious mode corresponding to the center-of-mass (c.m.) motion comes at zero excitation energy in the RPA. This condition determines the renormalization factor f for the residual interaction ($t_0 \to f \times t_0$ and $t_3 \to f \times t_3$). We obtain

MITSURU TOHYAMA AND TAKASHI NAKATSUKASA
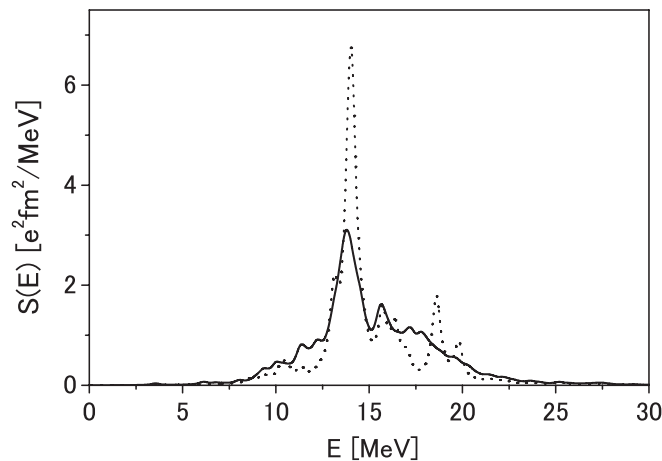
FIG. 1. Strength functions calculated in the SRPA (solid line) and RPA (dotted line) for ^{140}Ce. An artificial width $\Gamma = 0.5$ MeV is used for smoothing. See text for details.

$f = 0.73$ for ^{142}Nd, and similar values for other nuclei as well. Since the coupling between the spurious c.m. motion and 2p-2h configurations is weak, these renormalization factors may approximately produce zero energy in the SRPA as well. Thus, we use this interaction for the calculation of the matrices a, b, and c in Eq. (1). For the residual interaction for the matrix d, following a prescription in Ref. [20], we introduce a zero-range interaction $v_0 \delta^3(\boldsymbol{r} - \boldsymbol{r}')$ in addition to the original t_0 and t_3 terms, then, fix the parameter v_0 by approximately reproducing the excitation energy of the lowest 1^- state in ^{142}Nd ($v_0 = -570$ MeV fm^3). With these residual interactions in the given model space, the spurious mode appears at a small imaginary energy ($\omega^2 \approx -1$ MeV^2) in the SRPA.

To check the stability of the result, shown in the following, with respect to the number of 2p-2h configurations, we performed a calculation for ^{142}Nd, with a small number of the 2p-2h configurations, about 10% of the configurations used in the present work. Nevertheless, as long as the parameter v_0 is adjusted to reproduce the excitation energy of the first 1^- state, the final result for the low-energy dipole states is similar to the present one. Therefore, it is unlikely that the expansion of the 2p-2h space changes our final conclusion in the present Rapid Communication.

We first show the results for the GDR. The $E1$ strength functions, $S(E) \equiv \sum_n |\langle n|rY_{1\mu}|0\rangle|^2 \delta(E - E_n) = dB(E1; 1^- \rightarrow 0^+_{\mathrm{gs}})/dE$, calculated in the SRPA (solid line) and RPA (dotted line) for ^{140}Ce, ^{142}Nd, and ^{144}Sm are shown in Figs. 1, 2, and 3, respectively. We use the $E1$ operator with the recoil charges, Ne/A for protons and $-Ze/A$ for neutrons, for the calculation of $S(E)$. The obtained discrete strength functions are smoothed with a Lorentzian with a small width ($\Gamma = 0.5$ MeV). The energy-weighted strength summed up to 50 MeV exhausts 87% of the energy-weighted sum-rule value including the enhancement term arising from the momentum-dependent parts of the Skyrme interaction. The strength distributions of the GDRs in the SRPA are broadened, compared to the RPA, due to the coupling to the 2p-2h states. In the inset of Fig. 2, the total photoabsorption cross section (solid line) calculated in the SRPA is compared with the experimental
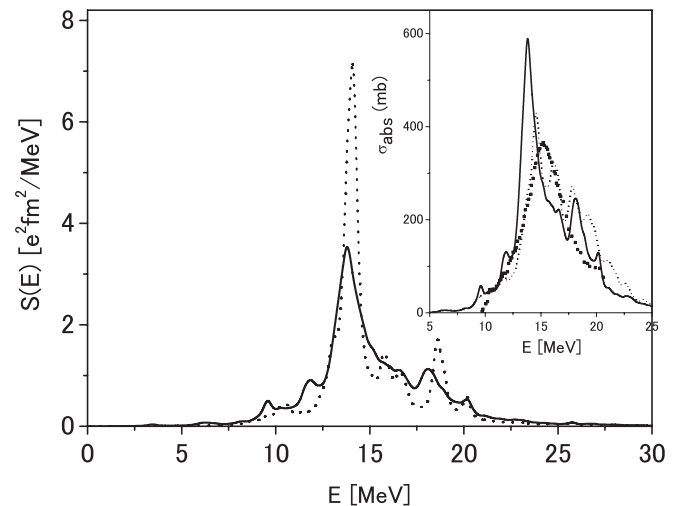

FIG. 2. Same as Fig. 1 but for ^{142}Nd. In the inset the total photoabsorption cross section calculated from the strength function in the SRPA (solid line) is compared with the experimental data (dots) [21]. The dotted line in the inset denotes the result calculated with $f = 0.9$.

data [21]. The shape of the GDR depends on the parameter f, whereas it is little affected by the parameter v_0. The GDR peak position and the profile are better described by a slightly larger value of f (see the dotted line in the inset of Fig. 2). Our calculation indicates that the coupling to the 2p-2h state induces an additional broadening due to the spreading width; however, the peak position is close to that obtained in the RPA calculation. This is very different from the recent SRPA calculation for ^{16}O in Ref. [22], which indicates a large shift of the GDR peak energy (more than 5 MeV) but almost no broadening. Although we do not fully understand the origin of this discrepancy, it may be due to the difference in the residual interactions. In Ref. [22], the residual interaction derived from the Skyrme energy functional was used for the SRPA calculation. We use the zero-range interaction with the renormalization factors, because it is not trivial to justify the use of the residual interactions derived from the Skyrme functional. For instance, the Skyrme energy
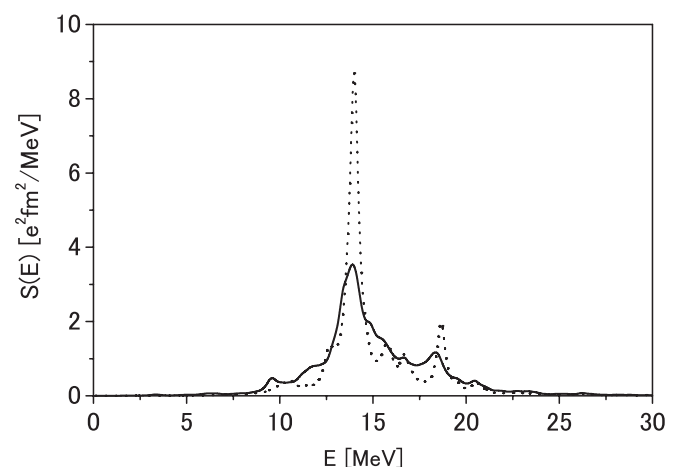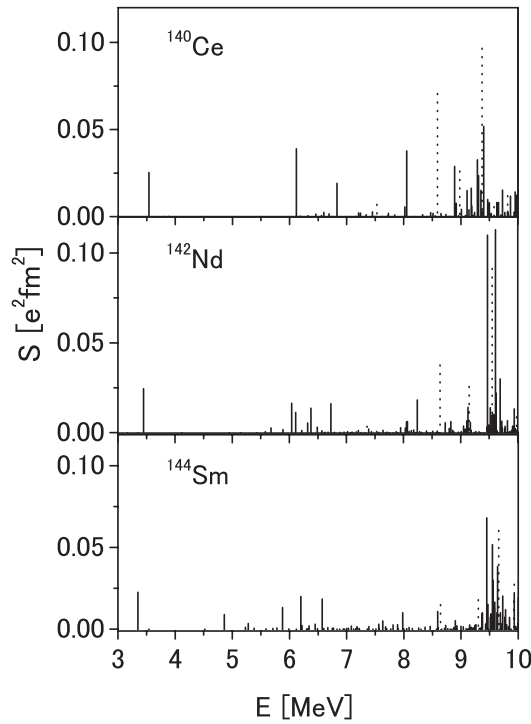

FIG. 3. Same as Fig. 1 but for ^{144}Sm.

FIG. 4. Low-energy $E1$ strength distributions, $B(E1; 1^- \rightarrow 0^+_{gs})$, calculated in the SRPA (solid line) and RPA (dotted line) for ^{140}Ce (top), ^{142}Nd (middle), and ^{144}Sm (bottom).

functionals are known to be incapable of describing nuclear pairing properties. Thus, if we directly adopt the interactions derived from the Skyrme functional in the 2p-2h space, it may produce unwanted spurious effects. More quantitative analysis of the GDRs require an improvement of the present calculation, especially, a self-consistent treatment of the residual interaction and the enlargement of the 2p-2h space.

Next, let us discuss the low-energy $E1$ strengths. In contrast to the GDR at high energy, the truncation of the 2p-2h configurations is supposed to be less serious. The $E1$ strengths, $B(E1) \downarrow$, below 10 MeV in ^{140}Ce, ^{142}Nd, and ^{144}Sm are shown in Fig. 4. In the RPA calculation, there is very little $E1$ strength in the energy region below 8 MeV, which agrees with the result of the QRPA calculation [16]. However, this is different from the findings [1–4]. In the SRPA calculation, the coupling to the 2p-2h configurations leads to a considerable $E1$ strength in this energy region. To make a quantitative comparison with experiment, the mean excitation energies and the summed $B(E1) \uparrow$ values for low-energy dipole states are calculated in the same way as in the experiment [3]: The mean energy is defined as $\bar{E} \equiv \sum E B(E1)/\sum B(E1)$, in which the summation is performed for the dipole states below 7.7 MeV for ^{140}Ce, those below 7.1 MeV for ^{142}Nd, and below 7.0 MeV for ^{144}Sm. The lowest 1_1^- states are excluded in the summation. The results are tabulated in Table I. For comparison, the RPA values, which include the lowest 1^- state, are listed in the table, but no 1^- state is predicted below 7.1 MeV for ^{142}Nd and ^{144}Sm. Although the calculated mean energies are slightly larger than the observed values, their isotone dependence is

TABLE I. Mean energies $\bar{E}$ and summed $B(E1) \uparrow$ values for the low-energy dipole states. The experimental values (Exp) are taken from Ref. [3]. See text for details.

Nucleus	$\bar{E}_x$ (MeV)			$\sum B(E1) \uparrow$ (e^2 fm^2)		
	RPA	SRPA	Exp	RPA	SRPA	Exp
^{140}Ce	7.53	6.47	6.28	0.021	0.219	0.308
^{142}Nd	–	6.31	6.07	0.0	0.224	0.184
^{144}Sm	–	6.04	5.69	0.0	0.233	0.208

consistent with the experiment and the summed transition probabilities are comparable to the experimental values [3].

In the RPA calculation, the neutron excitations are dominant in the low-lying states [14]. The present RPA calculation also indicates, for instance in ^{142}Nd, that the largest components of the low-lying dipole states located at $E_x = 7.36$, 8.64, 9.15, and 9.55 MeV are $(2p_{1/2} \rightarrow 2d_{3/2})\pi$, $(3s_{1/2} \rightarrow 3p_{3/2})\nu$, $(3s_{1/2} \rightarrow 3p_{3/2})\nu$, and $(3s_{1/2} \rightarrow 3p_{1/2})\nu$, respectively. In the SRPA, we see a significant fragmentation of the dipole strength into the energy range of $5 < E < 8$ MeV, in addition to the emergence of the lowest 1_1^- state at $E \approx 3.5$ MeV. Many of these low-lying dipole states have proton 2p-2h characters, such as $([1g_{7/2}2d_{5/2}]^{6^+} \rightarrow [1h_{11/2}2d_{3/2}]^{7^-})\pi$ and $([1g_{7/2}2d_{5/2}]^{6^+} \rightarrow [1h_{11/2}3s_{1/2}]^{5^-})\pi$. These proton 2p-2h configurations come down to the lower energy because of the coupling to the 2p-2h configurations consisting of the neutron 1p-1h transition from the $1h_{11/2}$ orbit to the $1h_{9/2}$ orbit and the proton 1p-1h transitions from the $1g_{7/2}$ orbit (or $2d_{5/2}$ orbit) to the $1h_{11/2}$ orbit: $\pi 1g_{7/2}\nu 1h_{11/2} \rightarrow \pi 1h_{11/2}\nu 1h_{9/2}$ and $\pi 2d_{5/2}\nu 1h_{11/2} \rightarrow \pi 1h_{11/2}\nu 1h_{9/2}$. We have confirmed the importance of these proton-neutron 2p-2h configurations by performing the SRPA calculation in a smaller 2p-2h space. The SRPA calculation with the neutron $1h$ orbits qualitatively produces the same result.

To investigate further the property of the low-energy dipole states, we also check the behavior of $D(r)$, which is defined as the $E1$ transition strength $\langle \mu |r Y_1|0\rangle$ without the integration over the radial coordinate r. For the main peak of the GDR, $D(r)$ shows a single-peak structure. On the other hand, the low-energy dipole states obtained by the RPA calculation show an oscillating pattern. However, in the SRPA calculation, none of the peaks below 7 MeV show oscillations, but they do exhibit similar behavior to that of the GDR. This gives another confirmation that the coupling to 2p-2h states significantly modifies properties of the low-energy dipole states.

Finally, let us discuss the property of the lowest 1^- state. The excitation energies and the reduced transition probabilities $B(E1) \uparrow$ of the 1_1^- states in ^{140}Ce, ^{142}Nd, and ^{144}Sm are compared with the experimental values [3] in Table II. The calculated excitation energies decrease with increasing proton number, which is consistent with the experiment. However, the SRPA calculations overestimate the $B(E1) \uparrow$ values by a factor of 2.7–3.5. The structure of the 1_1^- states in these nuclei is supposed to be predominantly of the two-phonon quadrupole-octupole character $2^+ \otimes 3^-$ [1,3]. However, in the present SRPA calculation, the 2p-2h configuration $([\pi 1g_{7/2}\nu 1h_{11/2}]^{1^-} \rightarrow [\pi 1h_{11/2}\nu 1h_{9/2}]^{2^+})$ is dominant

TABLE II. Excitation energies E and $B(E1; 0_{gs}^+ \rightarrow 1^-)$ of the lowest 1^- states. Note that the energy of the 1_1^- state in ^{142}Nd was approximately fitted by adjusting the parameter v_0. The experimental values (Exp) are taken from Ref. [3].

Nucleus	E (MeV)			$B(E1) \uparrow (e^2 \, \text{fm}^2)$		
	RPA	SRPA	Exp	RPA	SRPA	Exp
^{140}Ce	7.53	3.54	3.644	0.021	0.076	0.0217
^{142}Nd	7.36	3.45	3.424	0.010	0.074	0.0211
^{144}Sm	7.18	3.35	3.226	0.004	0.068	0.0248

in these 1_1^- states, which differs from the two-phonon $2^+ \otimes 3^-$ character. The pairing correlation, which is not taken into account in the present calculation, may play an important role for a better description of the two-phonon character of the 1_1^- states, because they are essential in the description of the lowest quadrupole and octupole states. Furthermore, it has been known that the SRPA fails to describe the collectivity of the two-phonon states [23]. This is because the next-leading terms in the two-phonon state are missing in the SRPA. These missing terms beyond the SRPA can be taken into account by introducing $X_{php'h'}$ amplitudes in Eq. (1). A general equation for the extended RPA formalism with the ground-state correlation is given in Ref. [24]. Another possible method to improve the description of the two-phonon states is the dressed-four-quasiparticle approach proposed in Ref. [25]. These are beyond the scope of the present work but of significant interest in future.

In summary, the fragmentation of the dipole strength in the $N = 82$ isotones, ^{142}Nd, ^{142}Nd, and ^{144}Sm, was studied using the second random-phase approximation. The SRPA successfully produces the spreading of the giant dipole resonance and the concentration of the dipole strength in the low-energy region, simultaneously. However, the transition strength of the first dipole state was overestimated in the SRPA, indicating the necessity of a more elaborate treatment for the states with two-phonon character. The calculation based on the extended RPA with ground-state correlations is of great interest and currently under progress.

[1] A. Zilges *et al.*, Phys. Lett. B **542**, 43 (2002).
[2] J. Enders *et al.*, Nucl. Phys. A **741**, 3 (2004).
[3] S. Volz *et al.*, Nucl. Phys. A **779**, 1 (2006).
[4] D. Savran *et al.*, Phys. Rev. Lett. **100**, 232501 (2008).
[5] R. Schwengner *et al.*, Phys. Rev. C **76**, 034321 (2007).
[6] J. Gibelin *et al.*, Phys. Rev. Lett. **101**, 212503 (2008).
[7] O. Wieland *et al.*, Phys. Rev. Lett. **102**, 092502 (2009).
[8] K. Yoshida and N. Van Giai, Phys. Rev. C **78**, 064316 (2008).
[9] D. Peña Arteaga and P. Ring, Phys. Rev. C **77**, 034317 (2008); D. Peña Arteaga, E. Khan and P. Ring, *ibid.* **79**, 034311 (2009).
[10] N. Paar, Y. F. Niu, D. Vretenar, and J. Meng, Phys. Rev. Lett. **103**, 032502 (2009).
[11] S. Ebata *et al.*, Phys. Rev. C **82**, 034306 (2010).
[12] T. Inakura, T. Nakatsukasa, and K. Yabana, Phys. Rev. C **84**, 021302 (2011).
[13] M. Martini, S. Peru, and M. Dupuis, Phys. Rev. C **83**, 034309 (2011).
[14] N. Paar, D. Vretenar, E. Khan, and G. Coló, Rep. Prog. Phys. **70**, 691 (2007).
[15] S. Goriely and E. Khan, Nucl. Phys. A **706**, 217 (2002).
[16] K. Yoshida and T. Nakatsukasa, Phys. Rev. C **83**, 021304(R) (2011).
[17] E. Litvinova, P. Ring, and V. Tselyaev, Phys. Rev. Lett. **105**, 022502 (2010).
[18] S. Drożdż, S. Nishizaki, J. Speth, and J. Wambach, Phys. Rep. **197**, 1 (1990).
[19] D. Gambacurta, M. Grasso, and F. Catara, Phys. Rev. C **84**, 034301 (2011).
[20] M. Tohyama, Phys. Rev. C **75**, 044310 (2007).
[21] P. Carlos, H. Beil, R. Bergere, A. Lepretre, and A. Veyssiere, Nucl. Phys. A **172**, 437 (1971).
[22] D. Gambacurta, M. Grasso, and F. Catara, Phys. Rev. C **81**, 054312 (2010).
[23] T. Tamura and T. Udagawa, Nucl. Phys. **53**, 33 (1964).
[24] M. Tohyama and P. Schuck, Eur. Phys. J. A **32**, 139 (2007).
[25] N. Kanesaki, T. Marumori, F. Sakata, and K. Takada, Prog. Theor. Phys. **49**, 181 (1973); **50**, 867 (1973).